The Plant Cell, Vol. 25: 3251–3265, September 2013, www.plantcell.org

RESEARCH ARTICLES

TED, an Autonomous and Rare Maize Transposon of the *Mutator* Superfamily with a High Gametophytic Excision Frequency[W]

Yubin Li,[a] Linda Harris,[b] and Hugo K. Dooner[a,c,1]

[a] Waksman Institute, Rutgers University, Piscataway, New Jersey 08854
[b] Agriculture and Agri-Food Canada, Ottawa, Ontario, Canada K1A 0C6
[c] Department of Plant Biology, Rutgers University, New Brunswick, New Jersey 08901

***Mutator* (*Mu*) elements, one of the most diverse superfamilies of DNA transposons, are found in all eukaryotic kingdoms, but are particularly numerous in plants. Most of the present knowledge on the transposition behavior of this superfamily comes from studies of the maize (*Zea mays*) *Mu* elements, whose transposition is mediated by the autonomous *Mutator-Don Robertson* (*MuDR*) element. Here, we describe the maize element *TED* (for *Transposon Ellen Dempsey*), an autonomous cousin that differs significantly from *MuDR*. Element excision and reinsertion appear to require both proteins encoded by *MuDR*, but only the single protein encoded by *TED*. Germinal excisions, rare with *MuDR*, are common with *TED*, but arise in one of the mitotic divisions of the gametophyte, rather than at meiosis. Instead, transposition-deficient elements arise at meiosis, suggesting that the double-strand breaks produced by element excision are repaired differently in mitosis and meiosis. Unlike *MuDR*, *TED* is a very low-copy transposon whose number and activity do not undergo dramatic changes upon inbreeding or outcrossing. Like *MuDR*, *TED* transposes mostly to unlinked sites and can form circular transposition products. Sequences closer to *TED* than to *MuDR* were detected only in the grasses, suggesting a rather recent evolutionary split from a common ancestor.**

INTRODUCTION

Though transposable elements (TEs) occupy a large fraction of most eukaryotic genomes and are major contributors to genome size evolution, the amplification of different TE superfamilies varies greatly from species to species (Kidwell, 2002; Wessler, 2006; Feschotte and Pritham, 2007; Ågren and Wright, 2011; Fedoroff, 2012). Among class 2 or DNA TEs (Wicker et al., 2007), the *Mutator* (*Mu*) superfamily has been particularly successful in colonizing plant genomes (Jiang et al., 2004; Holligan et al., 2006; Delseny et al., 2010; González and Deyholos, 2012), yet practically all knowledge of its transposition and regulation traces to genetic studies of the maize (*Zea mays*) *Mu* elements, the founding members of the superfamily (Robertson, 1978; Robertson and Stinard, 1989; Bennetzen, 1996; Walbot and Rudenko, 2002; Lisch and Jiang, 2009).

The autonomous maize *Mu* element *MuDR* (Chomet et al., 1991; Hershberger et al., 1991; Qin et al., 1991) controls the transposition of a diverse family of elements that share terminal inverted repeats (TIRs) but vary in internal sequence. *MuDR* encodes a Mutator Regulator A (MURA) protein with a highly conserved transposase domain (Hua-Van and Capy, 2008) and a MURB protein that has been implicated in element reinsertion, but whose function remains uncertain at this time (Lisch and Jiang, 2009). *Mu*-like elements (*MULE*s) have been reported in a number of other species besides maize (Lisch, 2002). Most are defective elements that would be incapable of autonomous transposition, but some encode intact proteins homologous to the MURA transposase, and a few have been shown to transpose autonomously: *Hop1* in *Fusarium oxysporum* (Chalvet et al., 2003), *Jittery* in maize (Xu et al., 2004), and *Os3378* in rice (*Oryza sativa*; Gao, 2012). Unlike *MuDR*, these autonomous elements do not encode a B function and, peculiarly, lack defective close relatives in their respective genomes. Here, we describe *TED* (for *Transposon Ellen Dempsey*), an autonomous maize *MULE* captured in the *bz* locus of a transposon-laden line (Rhoades and Dempsey, 1982). The resulting *bz-m175* mutable allele has enabled a detailed analysis of the transposition properties and behavior of this novel autonomous *MULE*, which differs from *MuDR* in a number of ways.

TED encodes a protein closely related to MURA that we have called TEDA, but no other protein, so all its *trans*-acting transposition properties are dependent on this one protein. Transposition-deficient derivatives that lose part or all of TEDA arise with a high frequency at meiosis. Unlike *MuDR*, *TED* is a very-low-copy-number element that is neither silenced by inbreeding nor amplified by outcrossing. *TED*'s unusually high transposition frequency in the gametophytic generation, particularly in the embryo sac, can account for most recovered *Bz*' germinal reversions. Like *MuDR*, *TED* transposes mostly to unlinked sites and forms circular transposition products of as yet unclear significance. Based on our reversion analysis of *bz-m175*, we infer that the double-strand breaks (DSBs) produced by *TED*

[1] Address correspondence to dooner@waksman.rutgers.edu.
The author responsible for distribution of materials integral to the findings presented in this article in accordance with the policy described in the Instructions for Authors (www.plantcell.org) is: Hugo K. Dooner (dooner@waksman.rutgers.edu).
[W] Online version contains Web-only data.
www.plantcell.org/cgi/doi/10.1105/tpc.113.116517

excision are repaired by nonhomologous end joining in the mitotic divisions of the sporophyte and gametophyte, but not at meiosis, where they appear to be repaired by DNA synthesis using the sister chromatid as template. Sequences more similar to *TED* than to *MuDR* were detected only in grass genomes, suggesting that these elements diverged only recently from a common ancestor.

RESULTS

Isolation and Genetic Behavior of *bz-m175*

The *bz-m175* mutable allele arose in an experiment designed to capture transposons in the maize stocks High Loss and High Knob (Rhoades and Dempsey, 1982), known to carry active elements from different superfamilies (Dennis et al., 1988; Shepherd et al., 1989). It conditions a uniformly fine-spotted bronze mutable (bz-mF) phenotype (Figure 1A), a telltale sign of a transposon mutation at *bz* that reverts late in aleurone development. In testcrosses of *Sh bz-m175/sh-bz-X3* hemizygotes, the bz-mF phenotype cosegregates with the plump phenotype conditioned by the *Sh* allele (see Supplemental Table 1 online), suggesting that the transposon in *bz-m175* acts autonomously.

The *bz-m175* allele has an obvious positive dosage effect on kernel spot number since the number of purple spots is twice as high when *bz-m175* is crossed as the maternal parent to a *bz* tester than in the reciprocal cross (see Supplemental Figures 1A and 1B online). Large somatic revertant sectors are sometimes seen in adult plant tissues, indicating that the transposon at *bz* also reverts late in sporophytic development (Figures 1B to 1F). Occasionally, very heavily spotted kernels can be found in segregating populations of *bz-m175* (see Supplemental Figure 1C online), but the phenotype is not heritable. The *bz-m175* allele has been backcrossed four times to a W22 *sh-bz-X3* stock without any obvious change in phenotype or apparent loss of activity.

The mutable *bz-m175* allele was isolated by PCR amplification from leaf DNA. Two PCR products were amplified from *bz-m175/bz-R* heterozygotes using primers spanning the *bz* coding region (Figure 2). The larger band was ~4 kb longer than either the progenitor band or somatic excision products. Sequence analysis of the large PCR product showed that *bz-m175* had

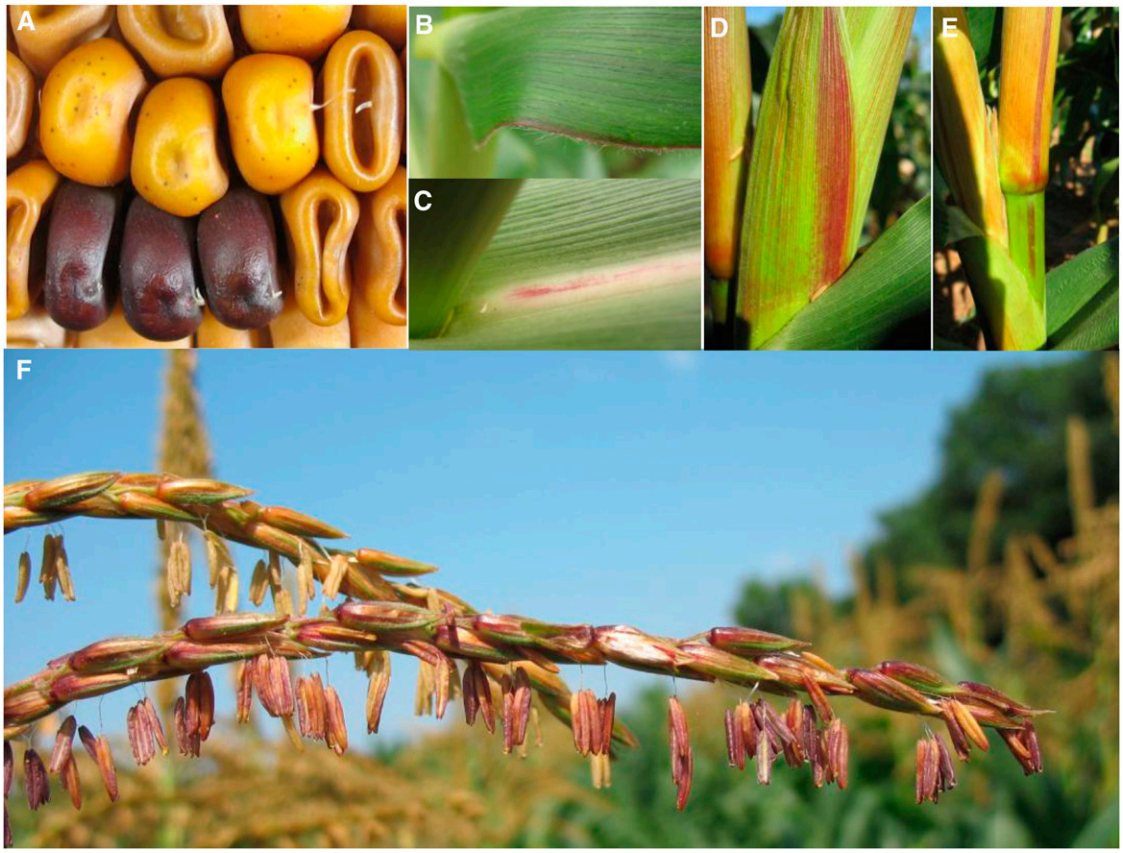

Figure 1. *bz-m175* Phenotypes.

The *bz-m175* allele conditions a uniformly fine-spotted mutable phenotype, as illustrated by the kernels in **(A)**. This ear sector also shows a rare cluster of premeiotic germinal Bz' purple revertants. Occasional large somatic sectors can also be seen in sporophytic tissues: leaf blade and midrib (**[B]** and **[C]**); husk **(D)**; culm and leaf sheath **(E)**; and tassel **(F)**.

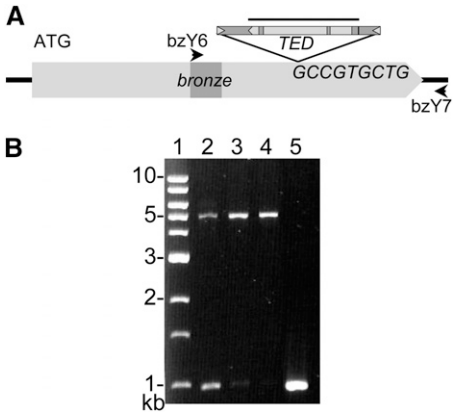

Figure 2. The *bz-m175* Allele.

(A) Structure of *bz-m175*, showing the *TED* element insertion in the *bz* second exon, the sequence of the 9-bp insertion site, and the location of primers bzY6 and bzY7 (arrows) and the TEDA hybridization probe (bar). *bz* exons and intron are light and dark gray, respectively. *TED* TIRs are triangles, and its coding and noncoding sequences are light and dark gray, respectively.

(B) Amplifications with bz-Y6 and bz-Y7 of the parental *TED* band and of somatic excision products from *bz-m175*. Lane 1, 1-kb DNA ladder; lane 2, *bz-m175* seeding leaf; lanes 3 and 4, *bz-m175* adult leaves; lane 5, *Bz-McC* wild-type control.

resulted from the insertion of a novel TE in the second *bz* exon. The element was named *TED*, for *Transposon Ellen Dempsey*, in honor of one of the discoverers of the High Loss stock.

Structure of *TED* and *TED*-Like Elements in Maize

TED is 3960- bp long, causes a 9-bp target site duplication (TSD) at the insertion site, and ends in 191-bp TIRs, which are 92.1% identical to each other. It is predicted to encode a 785–amino acid protein that we have denominated TEDA because of its homology to MURA, the *MuDR* transposase (51% identity; 67% similarity over 742 amino acids). *TED* does not share significant nucleotide sequence similarity with either *MUDR* or other known elements in the *Mu* superfamily, except over the third and largest exon of the transposase gene. Not surprisingly, the *TED* TIRs lack a MURA binding site sequence (Benito and Walbot, 1997).

No sequences with significant similarity to the *TED* TIRs were found in the B73 maize genome, which contains 155 *MULE* families (Schnable and al., 2009). However, B73 sequences distantly related to the TEDA coding region and flanked by distinct TIRs were detected by tBLASTn searches using the TEDA transposase as query. Homology of these sequences to *TED* was confirmed by DNA gel blot hybridization (see Supplemental Figure 2 online). Unlike most known *MULE*s other than *Jittery* (Xu et al., 2004), *TED* is an extremely low-copy TE. Among the 11 inbred lines examined, only H99, I137TN, and W22 contain a single copy of a *TED*-like element, but none of them have *TED* activity (see later section). TEDA-hybridizing bands with *TED* activity were only detected in the *bz-m175* progenitor line and in the original High Loss stocks of Rhoades and Dempsey.

Germinal Transposition of *TED* in *bz-m175*

In crosses of *bz-m175* females to a *bz* tester, purple kernels representing putative revertants (*Bz*') are recovered at a frequency of around one per 400 gametes (113/45,000). However, only two showed the concordant Bz endosperm and embryo phenotypes expected of meiotic reversion events (Figure 3A). One of them occurred as a single purple kernel on the ear and the other as a cluster of four kernels, reflecting an early premeiotic event. The majority (111/113) were class 1 nonconcordant reversion events (Bz endosperm; bz-m embryo), indicating a high *TED* excision activity in the female gametophyte. These reversions can arise in any one of four possible non-egg cell lineages (Figure 3B).

The high frequency of class 1 nonconcordant reversions (2.5×10^{-3}) prompted us to screen for the reciprocal nonconcordant reversions having a bz-m endosperm and a Bz embryo (class 2) among the same testcross progeny. This class can only arise from a *TED* excision that occurs at the last female gametophytic mitosis and is transmitted to the egg cell (Figure 3C), so its frequency is expected to be lower than that of class 1. The entire population of spotted kernels was germinated and screened for purple (Bz') seedlings. Eight Bz' revertants were identified and their heritability was confirmed by genetic test crosses. Their frequency, 1.8×10^{-4}, is considerably lower than that of the reciprocal nonconcordant class and four times greater than that of the concordant class, though the numbers are too low to establish significance.

The occurrence of *TED* excisions in the female gametophyte allows us to analyze the role in reinsertion of the single gene encoding the TEDA transposase. We found that *TED* reinsertion was high among *Bz*' germinal revertants (Figure 4A). Three new *TED*-hybridizing bands were detected among the two concordant excision events. The four clustered Bz' revertants share a reinsertion event (lanes 12 to 15), as expected from a premeiotic *TED* transposition, but one has an additional unique reinsertion that must have occurred at or after meiosis (lane 13). Two of the nonconcordant class 2 reversions showed new *TED* bands (lanes 18 and 23), indicating that *TED* reinserted in a fraction of the egg cells after excising in the last megagametophytic mitosis. The DNA gel blot observations were confirmed by isolating and sequencing the nine *TED* reinsertion sites (see Supplemental Table 2 online). Our female parent reversion data indicate that *TED* excision and reinsertion are much higher in the postmeiotic gametophytic mitoses than at meiosis or the premeiotic mitoses, though they appear to be differentially regulated in the different cell lineages of the embryo sac.

By contrast, purple kernel Bz' revertants are rarely recovered using *bz-m175* as the pollen parent. In a population of almost 100,000 gametes, only 13 single-kernel Bz' revertants were obtained. Thus, the overall reversion frequency of *bz-m175* on the male side (approximately one per 10,000 gametes) is 25-fold lower than on the female side. Ten revertants were concordant and could have arisen during microsporogenesis or at the first pollen mitosis (Figure 3D). Four reinsertion events were detected

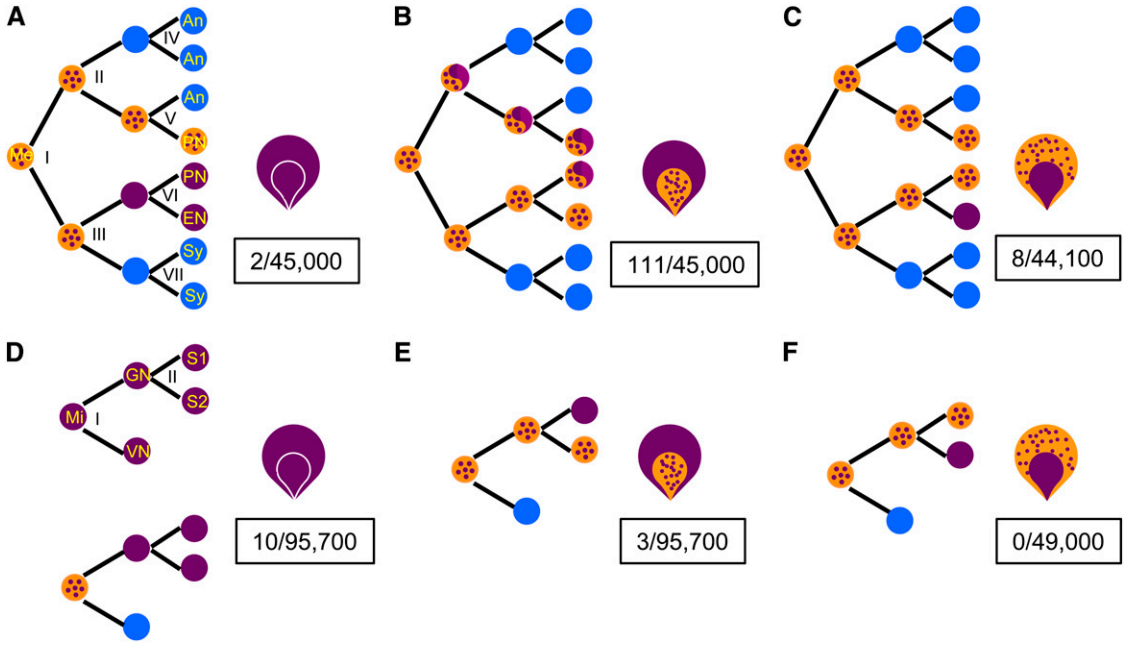

Figure 3. *bz-m175* Reversion in Female and Male.

Mitotic divisions and differentiated cells of the female and male gametophytes are identified in **(A)** and **(D)**, respectively. The exceptional kernel phenotypes produced in testcrosses of *bz-m175* as either maternal or paternal parent are inferred to arise by the reversion events diagrammed to their left. The frequencies of each kernel class are boxed. Light-blue closed circles are nuclei that do not affect these kernel phenotypes. Adapted from Dooner and Belachew (1989).

(A) to **(C)** Female gametophyte (embryo sac): Me, megaspore; An, antipodals; PN, polar nuclei; EN, egg nucleus; Sy, synergids.

(A) Concordant kernel (Bz endosperm and embryo) from Bz' reversion at megagametophytic mitosis I or at meiosis (data not shown).

(B) Class 1 nonconcordant kernel (Bz' endosperm and bz-m embryo) from postmeiotic Bz' reversion in four possible non-egg cell lineages.

(C) Class 2 nonconcordant kernel (bz-m endosperm and Bz' embryo) from postmeiotic Bz' reversion only in egg cell lineage.

(D) to **(F)** Male gametophyte (pollen): Mi, microspore; GN, generative nucleus; VN, vegetative (tube) nucleus; S1 and S2, sperm nuclei.

(D) Concordant kernels from meiotic Bz' reversion (top) or postmeiotic Bz' reversion in generative nucleus (bottom).

(E) Class 1 nonconcordant kernels from postmeiotic Bz' reversion in sperm fertilizing the central cell.

(F) Class 2 nonconcordant kernels from postmeiotic Bz' reversion in sperm fertilizing the egg.

among them (Figure 4A), a comparable reinsertion fraction to that observed in the egg cell. The remaining three revertants were nonconcordant, having originated most likely from the fertilization of the central cell of the embryo sac by a *Bz*' sperm cell that arose from a *TED* excision in the second pollen mitosis (Figure 3E). The reciprocal class 2 nonconcordant revertants (Figure 3F) were searched for in the same testcross progeny. Among 50,000 seedlings germinated from spotted seed, no such revertants were found, a result in agreement with the low frequency of the reciprocal nonconcordant class in the same cross. Taken together, the *bz-m175* reversion data indicate that *TED* transposition is much higher in the megagametophyte than in the microgametophyte.

All the *Bz*' revertants had the unique single-nucleotide and indel polymorphisms of the *Bz* progenitor of *bz-m175* (GenBank accession number KF279655), which was absent from the field of the reversion experiments, arguing that they did not arise from pollen contamination. None of the *Bz*' revertants from either reciprocal cross bore a transposon footprint, but unselected somatic excision products revealed multiple footprints (see below). This observation underscores the importance of the highly conserved UDP-Glc binding domain disrupted by *TED* for enzymatic activity of the *bz*-encoded flavonoid 3-*O*-glucosyltransferase (Offen et al., 2006).

Stable bz (*bz-s*) mutations are recovered about three times more frequently than Bz' revertants in crosses of *bz-m175* females to a *bz* pollen tester (48/7300). These derivatives most likely arise at or around meiosis because they occur as single kernels in the ear and their recessive bronze endosperm phenotype can only be produced if the two nuclei in the central cell, whose lineages separate at the first postmeiotic mitosis, are mutant (Dooner and Belachew, 1989). All 48 *bz-s* mutations arose from deletions in the *bz-m175* allele. Thirty (63%) carried internal *TED* deletions at the original site (Figure 5, 1 to 30). These are defective *TED* (*dTED*) nonautonomous elements, which can be activated by autonomous *TED* elements present elsewhere in the genome (see below). Because this class would not have been selected if a transposed *TED* had been retained in the genome, the true frequency of *bz*-s mutations from *bz-m175* is even higher. Three (6%) carried a *fractured TED* (*fTED*) element lacking one of the two ends and 15 (31%) carried *bronze* deletions of unknown size.

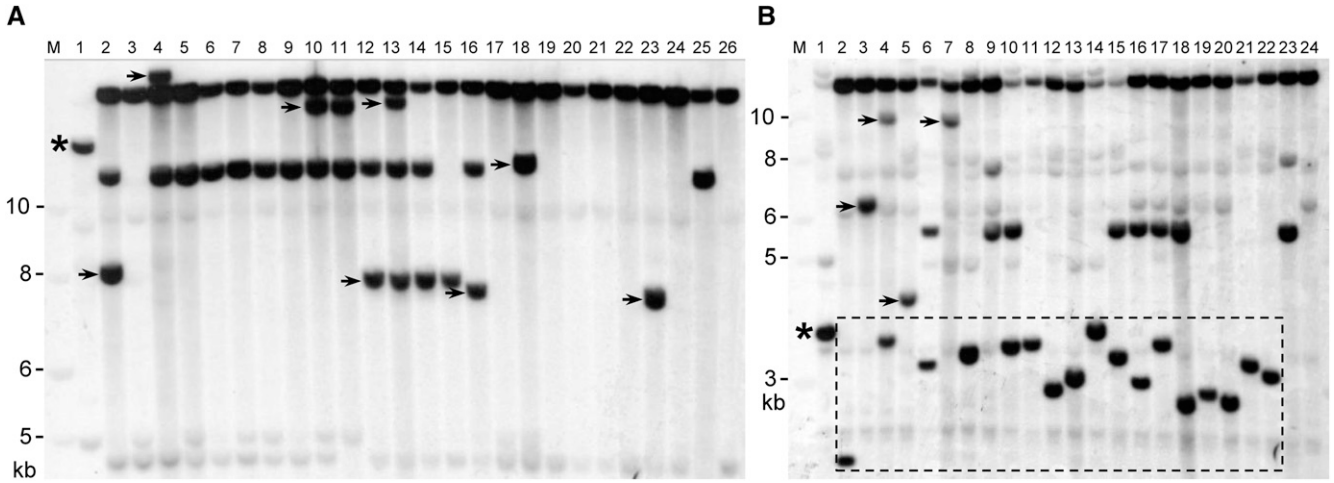

Figure 4. Detection of *TED* Transpositions.

(A) Bz' revertants of *bz-m175*. Lane 1, *bz-m175*; lanes 2 to 24, Bz' revertants; lane 25, *sh-bz-X2*; lane 26, *sh-bz-X3*. *Hin*dIII digest, TEDA probe.
(B) bz-s derivatives of *bz-m175* (dashed rectangle). Lane 1, *bz-m175*; lanes 2 to 22, bz-s derivatives with a defective or fractured *TED*; lane 23, *sh-bz-X2*; lane 24, *sh-bz-X3*. *Sac*I digest, TEDA probe.
Neither restriction enzyme cuts within the probe. *trTED* bands are marked with arrows and parental *bz-m175* bands with asterisks. The nonsegregating high molecular weight band is present in all W22 stocks and the segregating lower band (~12 kb in **[A]** and 5.5 kb in **[B]**) derives from the *sh-bz-X2* parent.

Different internal sequences have been deleted in the *dTED* elements. The deletions vary in size from 15 to 2240 bp and always include part of the TEDA coding region (210 to 3520), but never extend into the TIRs. In all cases, 2- to 8-bp short repeats flank the deletion endpoints (see Supplemental Table 3 online). Most deletions create premature stop codons that lead to nonfunctional transposases lacking the region coding for the conserved DDE triad domain (Hua-Van and Capy, 2008). Some deletions had filler DNA (4/30), as have been found in deletions from other transposons (Rubin and Levy, 1997; Yan et al., 1999;

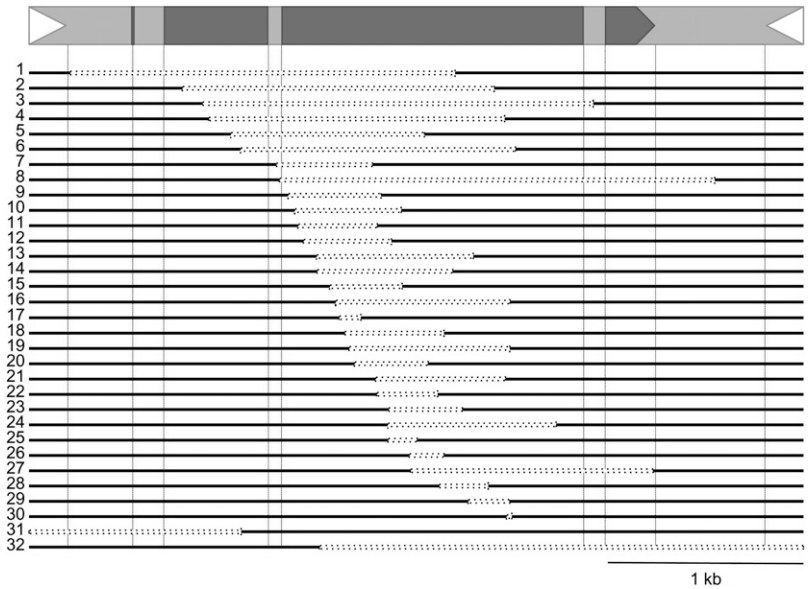

Figure 5. Structure of *dTED* and *fTED* Elements.

bz-s derivatives from *bz-m175*. 1 to 30, *dTED*s; 31 and 32, *fTED*s. Deletions are shown as dashed open bars. TIR locations and TEDA exon-intron junctions are indicated by vertical dashed lines. The *dTED20* derivative was used to assay the activity of *trTED* elements in segregation analyses (see Supplemental Figure 4 online).

Raizada et al., 2001; Conrad et al., 2007; Huang and Dooner, 2012) and in spontaneous deletions from different organisms (Roth et al., 1985; Wessler et al., 1990). The filler DNA varies in size from 8 to 66 bp and originates from nearby sequences located 23 to 109 bp from the deletion junction. The largest filler DNA, found in *dTED* element No. 5 consists of two unequal fragments, 30 bp apart in the original TED element and flanked by different short repeats.

Either end can be lost in the *fTED* elements. One of the two 5′ TIR deletions removes 1084 bp from the *TED* 5′ end and 34 bp of adjacent *bz* sequence and is flanked by a perfect 8-bp direct repeat in the *bz-m175* progenitor allele (see Supplemental Table 3 online, No. 31). A genetically active transposed *TED* (*trTED*) element was also detected in this line (data not shown). The other 5′ TIR deletion is much larger and extends into the distal *bz-stc1* intergenic region. The 3039-bp 3′ TIR deletion removes 2437 bp from the *TED* 3′ terminus and 602 bp of adjacent *bz* sequence (Figure 5, No. 32). Much larger deletions account for the remaining 15 *bz* deletion derivatives from *bz-m175*. Eleven of them contain a *trTED* element elsewhere in the genome (Figure 6), suggesting that *TED* often reinserts in the genome after germinal excision. The genetic analysis of bz-s derivatives is described in greater detail in the next section.

As with Bz′ selections, a few rare premeiotic events were detected among the bz-s selections. More frequently, the multiple bz-s kernels of the same cob arose from independent excision events, as evidenced by the different alleles carried by different kernels. In one case, five different *dTED* elements (see Supplemental Table 3 online, bz-s derivatives 5, 8, 11, 13, and 16) were found among six bz-s kernels from the same cob, the remaining one carrying a large *bz* deletion and a *trTED* element. The lack of perfect adjacent deletions (deletions immediately next to *TED*) and the particularly large size of some deletions distinguish *TED* from most other DNA transposon families but are reminiscent of changes brought about by *MuDR* (Hsia and Schnable, 1996).

Genetic Interaction of *trTEDs* and *dTEDs*

The bz-s selections containing *dTED* elements (Figure 5) can serve as reporter lines to test the transposition activities of the *trTED* elements identified molecularly among both Bz′ and bz-s selections from *bz-m175*. A 20 × 30 grid was set up to test simultaneously the respective abilities of the 20 *trTED* elements to reactivate *dTED* excision from *bz* and of the 30 *dTED* elements to be mobilized by a TEDA transposase provided in trans. The results of all hybrid combinations were uniformly positive:

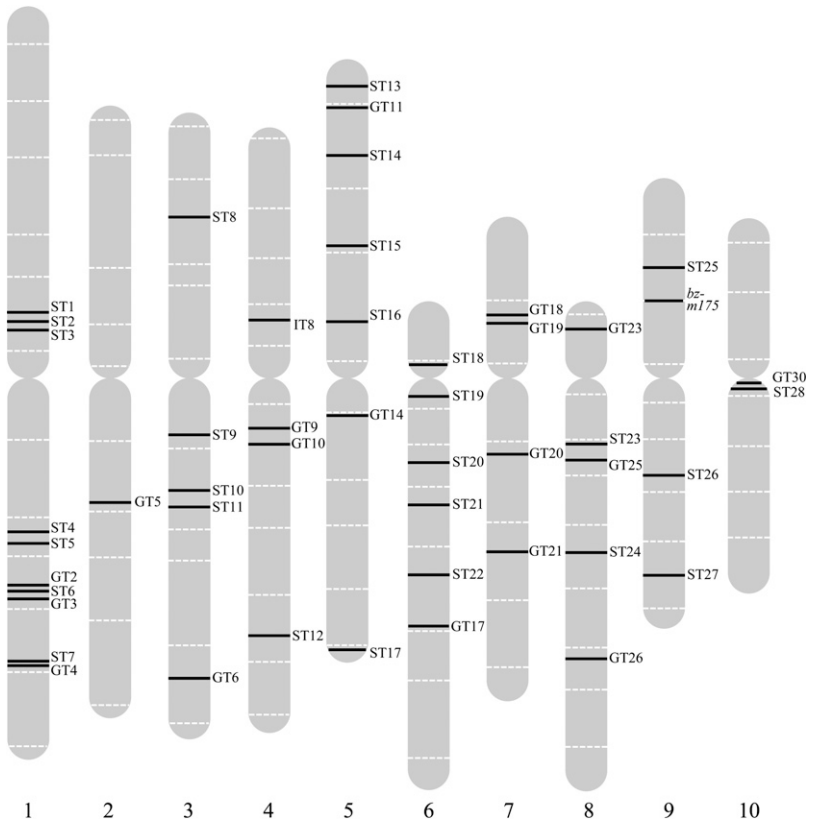

Figure 6. Location of *trTED*s in the Maize Genome.

*trTED*s were mapped to one of the maize pseudomolecules by BLAST searches of the B73 genome sequence with *TED*-adjacent sequences. ST, somatic transpositions; GT, germinal transpositions.

The 20 *trTED* elements were capable of *trans*-activating excision of the 30 new *dTED* elements at *bz*, producing in each case a spotting pattern indistinguishable from that of the *bz-m175* allele (see Supplemental Figure 3 online). *trTED* elements originally detected as new TEDA-hybridizing bands in a DNA gel blot (Figure 4) were always found to cosegregate with the spotting phenotype in crosses to *bz-m(dTED)* reporter lines (see Supplemental Figure 4 online). This indicates that *TED* generally retains its activity after transposing to new sites in the genome.

Nature and Distribution of *TED* Reinsertion Sites

To determine the nature of *TED* reinsertion sites, the DNA adjacent to the *trTED* elements was isolated and sequenced (see Supplemental Table 2 online). *TED* shows a strong preference for reinsertion in genic regions (16/18), as do other active *MULEs* (Fernandes et al., 2004; McCarty et al., 2005) and *Ac/Ds* (Cowperthwaite et al., 2002; Vollbrecht et al., 2010). Like its *Mu* cousin (Dietrich et al., 2002; May et al., 2003), *TED* displays a strong affinity for the 5′ end of genes (see Supplemental Figure 5 online). However, unlike *Mu* elements, which insert into a weak consensus sequence (Raizada et al., 2001), *TED* displays no obvious sequence preference. Occasionally, it transposes into low-copy repetitive sequences, yet it remains active. Since all *trTEDs* were first identified molecularly and then tested genetically, the latter observation suggests that *trTED*s retain their activity regardless of the nature of the reinsertion site.

Although most *TED* reinsertions were flanked by the 9-bp TSDs characteristic of *MULE*s (Walbot and Rudenko, 2002), some were not (see Supplemental Table 2 online). Two TSDs were 10 bp long and one was 6 bp long, sizes within the range of *MULE* TSDs that have been identified computationally (Singer et al., 2001). Germinal transpositions were mostly to unlinked sites distributed throughout the genome (Figure 6; see Supplemental Table 2 online), as are those of *MuDR* (Lisch et al., 1995) and *RescueMu* (Raizada et al., 2001) in maize and of At-*Mu1* in *Arabidopsis thaliana ddm1* mutants (Singer et al., 2001).

Somatic Transposition of *TED* in *bz-m175*

The rarity of large revertant sectors in the endosperm and sporophyte would suggest that *TED* excises only late in somatic development. However, a prominent PCR band corresponding in size to *TED* excision products was detected in *bz-m175* seedling leaves (Figure 2B). The wild-type-sized PCR products were cloned and sequenced to analyze the nature of the footprints resulting from somatic excision events. Fourteen different excision events (SE1 to SE14) were detected among 33 sequenced clones (see Supplemental Figure 6 online). Except for one +0 or no-footprint event (SE 9) and one 124-bp single-ended or *fractured TED* (*fTED*) element (SE 1), the majority were imperfect excisions of *TED* that left variable footprints, ranging from remnants of the transposon's TIRs and the host TSD (SE2 to SE8) to small deletions from either or both sides of the *bz* host sequence (SE10 to SE14). The different somatic excision events were recovered in widely variable frequencies, attesting to the heterogeneity of their timing. Most somatic excision sites did not show stretches of microhomology at the deletion junctions.

Nonstoichiometric TEDA-hybridizing bands, indicative of early somatic reinsertion events, were readily detected in DNA gel blots of *bz-m175* seedlings (see Supplemental Figure 7 online). A total of 29 somatic reinsertion sites were isolated from seedling DNA, sequenced, and mapped (see Supplemental Figure 5A and Supplemental Table 4 online). As in the germline, *TED* transposes preferentially into genic regions (23/29) scattered throughout the genome (Figure 6).

Molecular Characterization and Activity of *TED*-Like Elements in Other Maize Lines and Relatives

The *Bz* progenitor of *bz-m175* shares a prominent *TED*-hybridizing band with the High Loss ancestral lines (see Supplemental Figure 2 online). This band corresponds to a *TED*-like element inserted in the promoter region of a gene encoding a bHLH domain–like protein (see Supplemental Table 5 online, IT16). Two lines of evidence argue that this is the *TED* element that generated the *bz-m175* allele. First, the disappearance of this band in the original *bz-m175* isolate is coupled with the appearance of a new band corresponding to the *TED* insertion at *bz* (see Supplemental Figure 2 online). Second, the High Loss ancestor lines were shown to carry an active *TED* element in genetic *trans*-activation tests with the *bz-m(dTED)* tester lines described above.

Some of the maize inbred lines examined, such as W22, H99, and I137TN, show a strong *TED*-hybridizing band (see Supplemental Figure 2 online, lanes 5, 9, 10, and 11) that lacks genetic activity in crosses to *bz-m(dTED)* reporter lines. The *TED*-related elements had inserted in a genic sequence in H99, a conserved noncoding sequence in I137TN, and a MITE in W22 (see Supplemental Table 5 online). Their loss of activity may have resulted from either mutations in the element or from silencing by DNA methylation. Among maize relatives, *Zea nicaraguensis* (Iltis and Benz, 2000) shows the largest number of TEDA-hybridizing bands in DNA gel blots (see Supplemental Figure 2 online). Although *TED* activity of these elements was not tested, sequence comparison showed that they are highly similar to the maize *TED* element (see Supplemental Figure 8 online) so they may be transpositionally competent. As with the *trTED* elements from *bz-m175*, insertion sites in *Z. nicaraguensis* tend to correspond to genic regions (see Supplemental Table 5 online).

Duplicative Transposition

Some plants carrying a *tr-TED* (*bz-s/sh-bz-X3; tr-TED*/+) produced 50% more spotted kernels than expected in crosses with plants carrying a *bz-dTED* reporter (*bz-dTED/sh-bz-X3*). This observation suggests that a second unlinked *TED* element is present in the genome, most likely from duplicative secondary transposition of the *tr-TED*. The analysis of one example is shown in Supplemental Figure 9 online. GT20, a line bearing one *tr-TED* element, was crossed with two different *bz-dTED* lines, dTED2 and dTED17. The progeny from the GT20 × dTED2 cross shows the expected cosegregation of the spotted phenotype with both *tr-TED* with *dTED* (lanes 1 to 9). By contrast, in the GT20 × dTED17 cross (lanes 10 to 18), a second *TED*-

hybridizing band segregates among the spotted kernels (lanes 10 to 15). Only this band, but not the original *tr-TED*, is present in two spotted individuals (lanes 11 and 12), indicating that this is an active newly *tr-TED* element, arisen by duplicative transposition. Moreover, polymorphic, weaker hybridizing bands are observed in progenies from both crosses (12 bands among 18 individuals), suggesting that these *tr-TED*s can also undergo somatic duplicative transpositions.

Different duplicative transposition frequencies have been reported for members of the *Mu* family in maize, as high as 100% for *Mu* elements in a standard *Mu* line (Alleman and Freeling, 1986) and as low as ~6% for *Mu1* and 51.5% for *MuDR-1* in a Minimal Line (Lisch et al., 1995). To determine the duplicative transposition frequency of *TED*, we crossed 28 different plants of the GT20 line carrying a *trTED* to a *bz-dTED* reporter line. Fifteen of the crosses gave the expected 1/4 spotted kernels. However, the remaining 13 ears segregated 3/8 spotted kernels, a result consistent with two unlinked *TED* elements (see Supplemental Table 6 online). These data establish that the duplicative transposition frequency of *TED* is very comparable to that of *MuDR-1* elements (46% versus 51%) and that *TED* duplicative transpositions, like excisive ones, tend to be to unlinked sites.

Circular *TED* Elements

Maize *Mu* elements can exist in a circular extrachromosomal form (Sundaresan and Freeling, 1987). Circles covalently closed at the ends of the inverted repeats are also a feature of several other TEs (Curcio and Derbyshire, 2003). Although the *Mu* circles are not cleanly conjoined at the TIR ends and may contain deletions (V. Sundaresan, unpublished data; cited in Walbot and Rudenko, 2002), their presence exclusively in *Mu*-active lines suggests that they originate during the transposition process.

The similar preference of *Mu* and *TED* to transpose to unlinked genic sequences both germinally and somatically prompted us to search for circular-*TED* (*cTED*) DNA molecules in *bz-m175* somatic tissues. We performed PCR on *TED*-active lines with divergent *TED* internal primers that would generate a product only if a circular DNA molecule was present (Figure 7A). In all cases, we readily detected PCR bands of the size expected of a *TED* element circularized by the end joining of its TIRs (Figures 7B to 7D) and cloned them for sequence analysis.

Simple head-to-head fusions of the two TIRs would create new palindromic restriction sites for *Ava*I, *Xho*I, and *Bcg*I, but these were not found. This indicates that the fusion of the two ends was more complex, as had been found for *Mu* circles (Sundaresan and Freeling, 1987). Sequencing of the PCR products revealed that all had the expected inverted configuration of 5′ and 3′ends fused head-to-head. However, due to the high sequence identity of the TIRs, mixed reads from both sequencing directions were obtained in the TIR regions. With the aim of sequencing one TIR end at a time, the cloned PCR products were digested at sites unique to each TIR. This allowed us, in most cases, to read the sequences to within 80 bp from the TIR ends (see Supplemental Figure 10 online).

PCR products of sizes other than expected, indicative of rearrangements, were also sequenced. Some had truncations of either or both ends at the junctions, the deletions ranging from <100 to >2 kb (see Supplemental Table 7 online). Others had internal deletions, flanked by imperfect direct repeats, suggesting possible microhomology-mediated deletions (McVey and Lee, 2008) prior to circularization.

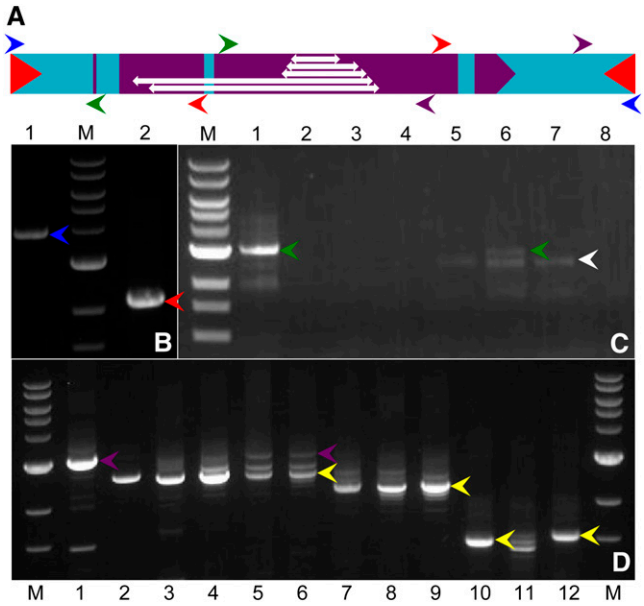

Figure 7. PCR Amplification of *cTED* and *dTED* from *bz-m175*.

(A) Color-coded PCR primers in the parental *TED* sequence. *dTED* deletions are shown as double-headed arrows (from top to bottom, *dTED20*, *dTED18*, *dTED13*, *dTED2*, and *dTED4*).
(B) Amplification of *bz-m175* DNA. Lane 1, a TIR single primer (blue arrows in **[A]**) amplifies the full-length element (blue arrowhead); lane 2, divergent internal primers (red arrows in **[A]**) produce a band of the expected size for a circular element (red arrowhead).
(C) Amplification with *TED* divergent primers (green arrows in **[A]**) of *cTED* and *dTED* elements (green and white arrowheads, respectively) in the *trTED* line GT30 (lane1) and in the bz-m progeny from a GT30 × *dTED20* cross (lanes 5 to 7). No products are amplified in the *TED*-minus bz progeny from the same cross (lanes 2 to 4) or in the *dTED20* line (lane 8).
(D) Amplifications with *TED* primers (purple arrows in **[A]**) of *cTED (*purple arrowheads) and corresponding *dTED* products (yellow arrowheads) from *bz-m175/bz-R* (lane 1) and four different *trTED/dTED* segregating lines. Lanes 2 to 6, *dTED18*; lanes 7 to 9, *dTED13*; lane 10, *dTED2*; lanes 11 and 12, *dTED4*; M, 1-kb DNA ladder.

dTED elements can form circular molecules, as well, but only if an active *TED* element is present. A population segregating for both *trTED* and *dTED* elements (GT30 and *dTED20*) was analyzed by inverse PCR using primers spanning the deletion in *dTED* (Figure 7A). These primers give rise to *TED* and *dTED* PCR products of different size, consistent with the internal 378-bp deletion that distinguishes the active and defective *TED* elements. We detected the predicted circular *TED* and *dTED* PCR products in active *TED* lines, but not in lines without *TED* activity (Figure 7C). Sequence analysis confirmed that the amplified PCR products were *cTED* and *cdTED* elements because they differed precisely at the site of the *dTED20* deletion junction. As

with *cTED* elements, end deletions of various sizes were found among *cdTED20* elements (see Supplemental Table 7 online). Circular excision products were also formed in four other populations segregating *dTED* and *trTED* elements (Figure 7D; see Supplemental Table 7 online).

TED-Like Elements in Sequenced Plant Genomes

Five autonomous *Mu* transposons have been identified so far: *MUDR* (Chomet et al., 1991; Hershberger et al., 1991; Qin et al., 1991), *Jittery* (Xu et al., 2004), *Hop* (Chalvet et al., 2003), *Os3378* (Gao, 2012), and *TED*. To investigate the distribution of *TED*-related elements in other plant genomes, we performed BLAST searches of plant sequence databases using the *TED* sequence as query.

Six sequences were found in the B73 maize genome. These probably correspond to the weakly hybridizing TEDA bands seen in DNA gel blots (see Supplemental Figure 2 online). All six sequences have typical *MULE* transposon features: They end in TIRs that vary in length from 115 to 186 bp and are flanked by 9-to 10-bp TSDs (see Supplemental Table 8 online). TIR identities vary from 82 to 99% within elements and from 77 to 99% between elements. However, the identities of these TIRs with *TED*'s were lower (75 to 79%), being restricted to a <90-bp region. Some of them are truncated copies of others (for instance, TEDLZm4 derives from TEDLZm2 by two separate short deletions; TEDLZm5 derives from TEDLZm2 by a single long deletion).

TEDA-hybridizing bands were also detected in sorghum (*Sorghum bicolor*), which is not surprising given its close relationship with maize. A BLASTN search of the sorghum genome sequence with *TEDA* as query identified five *MULE*s encoding transposases more similar to TEDA than to MURA (see Supplemental Figure 11 online). All five elements were closer to each other than to *TED*, indicating that they amplified after the sorghum-maize split 11.9 million years ago (Swigonová et al., 2004). The sorghum *TED*-like elements measure ~4.6 kb, end in ~200-bp TIRs of ~95% sequence identity, and are flanked by 9- to 10-bp TSDs (see Supplemental Table 8 online). None of them encodes a MURB-like protein. The *Brachypodium* genome also contains a *MULE* element more closely related to *TED* than to *MuDR*. However, in phylogenetic comparisons with other plant *MULE* transposases, TEDA was found to be closer to MURA than to most other annotated plant sequences (see Supplemental Figure 11 online).

DISCUSSION

Relationship to *MuDR* and *Mu* System

Here, we describe the *TED* element of maize, the founding member of a novel family of very-low-copy-number transposons within the *Mu* superfamily. *TED* was recovered from the *bz-m175* mutable allele in a High Loss stock known to undergo frequent chromosome breaks most likely because of its high content of active transposons (Rhoades and Dempsey, 1982). *bz-m175* was subsequently introgressed by repeated backcrossing into the genetic background of the inbred W22 without any change in phenotype, loss of activity, or large increase in *TED* copy number. In this respect, *TED* resembles the minimal *Mu* line (Lisch, 2002) rather than the original higher *MuDR* copy number lines, where *Mu* activity was silenced by inbreeding (Robertson, 1986) and *Mu1* copies greatly amplified by outcrossing (Alleman and Freeling, 1986).

TED and *TED*-like elements occur in the genus *Zea* and in close grass relatives, such as *Tripsacum*, *Sorghum*, and *Brachypodium*. These elements have the typical characteristics of a *MULE*: They encode transposases with homology to the *Mu* MURA protein, end in long inverted repeats of ~200 bp, and cause a 9-bp duplication of the host insertion sites (Figure 2). *TED* is the third characterized autonomous transposon of the *Mu* superfamily in maize, a model system unique in its number of genetically defined elements. Based on its transposase homology, *TED* is much closer to *MuDR* (Eisen et al., 1994; Hershberger et al., 1995) than to *Jittery* (Xu et al., 2004), an active *MULE* related to the phytochrome A transcription factors FHY3/FAR1 (Hudson et al., 2003). A phylogenetic comparison of *TED*-related elements in maize and other sequenced grasses reveals a disproportionate abundance of *TED*-like elements in *S. bicolor* and *Panicum virgatum*, suggesting that the *TED* family has amplified differentially in different plant genomes (see Supplemental Figure 11 online). Similar observations have been made for retrotransposons (Vitte and Bennetzen, 2006) and other DNA transposons, such as *PACK-MULE*s (Jiang et al., 2004) and *Helitrons* (Du et al., 2009; Li and Dooner, 2012).

Absence of a *B* Function

Despite the similarities among members of the *Mu* superfamily from different plant species, only *MuDR* encodes a MURB protein. The initial analysis of *MuDR* deletion derivatives suggested that this protein may be required for somatic and germinal insertion (Lisch et al., 1999), but to this day its function remains elusive (Lisch and Jiang, 2009). *TED* is the closest autonomous relative of *MuDR* found to date (see Supplemental Figure 11 online). It is fully transposition competent, being capable of both excision and reinsertion in somatic and germinal tissues, but it lacks a B function, like other autonomous *MULE*s of widely divergent phylogenetic origins: *Jittery* of maize (Xu et al., 2004), *Os3378* of rice (Gao, 2012), and *Hop* of *Fusarium* (Chalvet et al., 2003). These data argue that, if MURB is indeed required for *MuDR* reinsertion, that requirement evolved recently, after the separation of the MURA and TEDA clades.

Transposition in Sporophyte and Gametophyte

In contrast with *Mu* elements, which excise only late in development (McCarty et al., 1989; Raizada et al., 2001), *TED* can excise in young sporophytic tissues. PCR somatic excision products were more abundant in seedling leaves than in mature leaves (Figure 2). Although large revertant sectors are occasionally observed (Figures 1B to 1D), indicating an excision early in development, most reversions occur in the last few cell divisions, as in the *MuDR* system. However, whereas the timing of somatic excisions is not affected by dosage of the autonomous

element in either system, the frequency of somatic excisions in the aleurone shows a positive response to *TED* dosage (see Supplemental Figures 1A and 1B online).

Our analysis of putative germinal revertants of *bz-m175* uncovered an unusual *TED* feature, a high transposition frequency in the haploid gametophyte that can account for the majority of heritable excisions. In this respect, *TED* resembles the *hobo-Activator-Tam2* (*hAT*) elements *Inhibitor of R* of maize and *Tag1* of *Arabidopsis thaliana*, which excise in developing gametophytes, leading to a high frequency of germinal reversions (Williams et al., 1984; Eggleston et al., 1995; Galli et al., 2003), but differs from the majority of *Arabidopsis* transposons, which are transcribed and transpose in the pollen vegetative nucleus, but not in the sperm nuclei (Slotkin et al., 2009). Even though plants alternate between a diploid and a haploid phase, most genetic analysis in higher plants is performed with the dominant diploid sporophytic generation. Two properties of the *bz-m175* mutable allele allow our genetic analysis to extend to the haploid gametophytic generation. First, the *bz* gene is expressed both in the endosperm and the embryo/seedling, plant parts produced from the separate fertilization events of the central cell and egg cell in the female gametophyte by the two sperm in the male gametophyte. Second, *bz* affects anthocyanin pigmentation, a most readily scorable trait in these tissues.

Putative germinal revertants can be identified as fully purple kernels in *bz-m175* testcross ears (Figure 1A). The frequency of such kernels when using *bz-m175* as female parent (2.5×10^{-3}) is ~100-fold higher than the reversion frequency of *Mu1*-containing mutable alleles (Bennetzen, 1996; Walbot and Rudenko, 2002). However, most of these Bz kernels (111/113) have a bz-m embryo (i.e., they do not represent germinal events transmissible to the next generation). These class 1 nonconcordant kernels can arise from reversion events in four of the seven mitoses that lead to the formation of the mature haploid female gametophyte or embryo sac: divisions I, II, V, or VI (Figure 3B). We infer that reversions occur at the two- or four-nucleate stage of the embryo sac because concordant kernels would have been more numerous if reversions had occurred at the one-nucleate stage (division I) and had an equal probability of being incorporated into either daughter cell. The reciprocal class 2 nonconcordant kernels, with a bz-m endosperm and a Bz embryo (Figure 3C), can only arise from a reversion event that is transmitted to the egg cell in the last embryo sac mitosis (division VI) and was recovered at a substantially lower frequency (1.8×10^{-4} versus 2.5×10^{-3}). If a *Bz*' reversion at this mitotic division has an equal probability of being incorporated into the sib polar nucleus, then it can account for only eight of the 111 class 1 nonconcordant kernels (Bz' endosperm/bz-m embryo). This suggests that most reversions that produce class 1 nonconcordant kernels occur at mitotic divisions II or V in the embryo sac (Figure 3B) and, therefore, that *TED* excision in the haploid female gametophyte is under tight developmental control, as it is in the diploid sporophyte.

The frequency of concordant revertant kernels obtained in testcrosses using *bz-m175* as pollen parent is 1×10^{-4}, of the same order of magnitude as in the reciprocal cross. In the male gametophyte, the two sperm that participate in the double fertilization of the egg and central cell of the embryo sac share a common lineage until the last mitosis. Hence, concordant kernels can arise from reversion events either at meiosis or at the first pollen mitosis (Figure 3D). The reciprocal classes of nonconcordant kernels arise from reversion events at the second pollen mitosis and would be expected in roughly equal numbers, assuming no preferential fertilization by either sperm. As seen in Figures 3E and 3F, they occur in very low frequencies that do not differ significantly from each other.

All germinal *Bz'* revertants alleles, regardless of parent of origin, carry a +0 footprint, reflecting the importance of the *TED* insertion site for *bz* gene function, as *TED* disrupts the sugar nucleotide binding site deemed essential for the glucosyltransferase activity of the BZ protein (Hughes and Hughes, 1994; Offen et al., 2006). No simple excisions were detected among stable *bronze* alleles. In this class, *dTED* elements of different sizes predominate, followed by *bz* deletions large enough to remove at least one of the PCR priming sites flanking *bz* and by a small fraction of *fTED* elements resulting from a deletion of one end of the inserted *TED* element plus adjacent *bz* sequences.

Like *MuDR* and nonautonomous *Mu* elements (Lisch et al., 1995), *TED* is capable of somatic as well as germinal reinsertion. In this, it differs from *Jittery*, an unusual *MULE* that can excise but not reinsert in the maize genome (Xu et al., 2004). Both somatic and germinal transpositions are mainly to unlinked sites and show preference for the 5′ end of targeted genes, including the upstream promoter region and the first few exons (see Supplemental Tables 2 and 4 and Supplemental Figure 5 online; Figure 6), properties also evidenced by *Mu* elements (Dietrich et al., 2002; May et al., 2003; McCarty et al., 2005).

Excisive versus Duplicative Transposition during Development

Like other plant transposons (Walbot and Rudenko, 2002; Li and Dooner, 2009; Lisch and Jiang, 2009; Huang and Dooner, 2012), *TED* can undergo both excisive and duplicative transposition. Appearance of the transposon at a new site is accompanied in the former by complete loss of the transposon from the original site and in the latter by retention of the transposon in whole or in part at the original site. Thus, the two types of transposition can be empirically distinguished by the nature of the novel products formed at the original insertion site: simple excision footprints in the former and defective elements in the latter.

Simple excision footprints contain remnants of the TSD generated by transposon insertion. Most transposon excision footprints in plants lack stretches of microhomology greater than 3 bp at the new deletion junction and are taken to arise by nonhomologous end joining of the DSB produced by element excision (Daley et al., 2005). A few show longer stretches of microhomology ($\geq$ 5 bp) with filler DNA at the deletion junction sometimes and may arise by the rarer microhomology-mediated end joining repair of DSBs (McVey and Lee, 2008). Duplicative transpositions have been postulated to arise from replication repair of the DSB at the transposon excision site using either a sister or nonsister chromatid as template (Nassif et al., 1994). In this mechanism, incomplete repair would lead to variable deletions of the element at the donor site. Internally or terminally deleted elements found at the previous insertion site of

autonomous elements often have microhomology and filler DNA at the deletion junction. Such elements occur at a high frequency in the progeny of *bz-m175* plants.

Recessive stable mutations from unstable alleles occurring as single kernels in an ear can only arise at or around meiosis (Dooner and Belachew, 1989). Down-selection for stable bronze (bz-s) derivatives from *bz-m175* revealed an unexpectedly high frequency of different classes of deletion mutations resulting from *TED* transposition. Defective *TED* (*dTED*) elements (i.e., *TED* internal deletions that did not alter the host gene) were the most frequent class (62.5% of all mutations), large deletions extending bidirectionally into the host gene for at least 6 kb were half as frequent, and fractured *TED* (*fTED*) elements or deletions of one end of *TED* that extended unidirectionally into the host gene were one-tenth as frequent.

Strikingly, no simple excision footprints were recovered among the 48 bz-s germinal derivatives. Given that *TED* excision in somatic tissues results in simple footprints and that practically all of them would have produced a stable bronze phenotype, we conclude that, unlike in somatic tissues, double-stranded gap repair is most probably the only mechanism for repairing *TED*-induced DSBs in meiotic cells. The short direct repeats flanking the deletion junctions in *dTED* and *fTED* elements and the filler DNA sequences in a subset of them can be best explained by repair synthesis using the sister chromatid as template (Nassif et al., 1994). The deletion of the entire *bz* region in the *sh-bz-X2* homolog precludes the use of a nonsister chromatid as alternative template. The large bidirectional deletions of the host gene that can arise from *TED* excision have not been reported among mutable alleles carrying *Mu* elements, although in this study they were relatively frequent (2×10^{-3}). Their absence from *Mu* alleles could be simply due to the fact that only a few loss-of-function mutations have been studied. However, many down-selections of mutable alleles carrying *Ac*/*Ds* transposons have been analyzed (e.g., Huang and Dooner, 2012) without uncovering large deletions. Since the predominant mechanisms of DSB repair in germinal tissues differ between *hAT* and *Mu* elements, it is conceivable that large bidirectional deletions may be a general feature distinguishing these two transposon superfamilies.

Plant DNA transposons can also differ in the relative frequencies with which the two types of transposition occur in different tissues. Whereas *hAT* elements, like *Ac*, exhibit predominantly excisive transposition in both somatic (Kunze and Weil, 2002) and meiotic (Huang and Dooner, 2012) tissues, *Mu* elements undergo mainly excisive transposition in somatic cells (Britt and Walbot, 1991; Doseff et al., 1991) and duplicative transposition in meiotic cells (Schnable et al., 1989; Britt and Walbot, 1991; Doseff et al., 1991; Lisch and Jiang, 2009). In this respect, *TED* shows a similar behavior to *Mu* (Figures 3 and 6). However, the frequency with which defective elements are formed at a specific site appears to be higher for *TED* than for *Mu* (Hsia and Schnable, 1996), even though *Mu* duplicative transposition can be as high as one event per element per generation (Alleman and Freeling, 1986). This observation suggests that replication repair of the DSB induced by element excision aborts prematurely, leading to the synthesis of an incomplete element, more frequently with *TED* than with *Mu*.

Circular Transposition Products

Putative extrachromosomal transposition intermediates in the form of linear or circular DNA have been reported for the *Tc3* and *Tc1* elements of *Caenorhabditis elegans* (Radice and Emmons, 1993; van Luenen et al., 1993). In maize, extrachromosomal *Mu1* circular molecules were detected more than two decades ago (Sundaresan and Freeling, 1987), but their detailed structure was not resolved and, to this day, their biological significance remains unclear. Circularized *Ds* elements have also been reported in maize and in transgenic tobacco (*Nicotiana tabacum*; Gorbunova and Levy, 1997, 2000). On the other hand, no extrachromosomal circles were detected in *ddm1* mutants of *Arabidopsis*, in which normally quiescent *Mu* elements were demethylated and activated (Singer et al., 2001), leading the authors to suggest that circular forms could be transposition intermediates that require the MURB function found only in maize. Here, we provide evidence for the formation of circular *cTED* molecules in *bz-m175* plants and show that the formation of circular *cdTED* molecules occurs only in the presence of an autonomous *TED* element.

Using a PCR strategy, we have shown that *TED*/*dTED* excisions are accompanied by the formation of products with the expected size and joined TIR structure of extrachromosomal circular forms (Figure 7). Sequence analysis confirmed the head-to-head fusion structure and restriction analysis of the PCR products established that the fusions were not perfect, as the fragments lacked the restriction site at the junction predicted from precise joining of the transposon ends. Sequencing of PCR products with a shorter than expected length revealed deletions of variable sizes at the TIR joints (see Supplemental Table 7 online), in agreement with earlier findings in the *Tc1* and *Ac*/*Ds* systems. The TIR head-to-head fusions are most likely free of adjacent TSD sequences, as the junction sites of the circularized elements share no sequence similarity with the TSD sequences at the donor site.

The formation of circular extrachromosomal transposon molecules only in the presence of an autonomous *TED* element establishes that these molecules are indeed the products of transposition reactions. Whether they are true transposition intermediates can only be conjectural at this time. The observation that *TED*, like *Mu* elements, transposes mostly to unlinked sites, in contrast with *Ac*/*Ds*, argues that the *TED* donor and recipient sites do not associate physically during the transposition reaction and favors the view of an extrachromosomal transposition intermediate. However, none of the observed products had a perfect head-to-head fusion structure, suggesting that they may represent abortive transposition intermediates that are incapable of reinsertion and accumulate in the cell. Possibly, the true transposition intermediates are short-lived linear *TED* structures with TIRs bound by transposase molecules that protect them from exonucleolytic degradation.

METHODS

Genetic Stocks

The following genetic stocks were used: *bz-m175*, a mutable allele with a fine-spotted phenotype arisen in a High Loss × High Knob genetic

background (Rhoades and Dempsey, 1982); *sh-bz-X2* and *sh-bz-X3* (shrunken, bronze), x-ray–induced deletions of large chromosomal fragments extending beyond the 2-centimorgan *sh-bz* interval (Mottinger, 1973); and *bz-R*, the stable reference allele harboring a 340-bp deletion of *bz* coding sequences (Ralston et al., 1987).

Selection and Analysis of Bz′ and bz-s Derivatives

Bz′ germinal revertants were isolated from reciprocal testcrosses of *Sh bz-m175*/*sh-bz-X2* hemizygotes to *sh-bz-X3*. In these crosses, exceptional plump, purple kernels represent Bz′ derivatives from *bz-m175*. In the same populations, nonconcordant Bz' germinal revertants were screened by seedling phenotype (red coleoptile and leaf tips) after planting spotted kernels in sand benches in the greenhouse. All selections were self-pollinated and backcrossed to *sh-bz-X3*. bz-s stable bronze derivatives were obtained from testcrosses of *Sh bz-m175*/*sh-bz-X2* hemizygotes to *sh-bz-X3*. Putative bz-s derivatives were selected as plump, stable bronze kernels, self-pollinated, and backcrossed to *sh-bz-X3*.

DNA Isolation and DNA Gel Blot Analysis

Maize (*Zea mays*) genomic DNA was isolated from seedling, adult leaf tissues, and pollen as described (Li et al., 2013). Restriction digested DNA (10 μg) was resolved on 0.6% agarose gels and transferred to Hybond XL nylon membranes (Amersham Biosciences). ^{32}P-labeled probes were generated with Ready-To-Go DNA labeling beads (Amersham Biosciences). Hybridization and washing were performed according to the manufacturer's instructions. The 2814-bp TEDA probe was amplified from a genomic clone using primers spanning the coding region of the TEDA gene. The 1157-bp *bz* probe was amplified from a genomic clone using primers spanning the *bz* coding region upstream of the *TED* insertion site.

PCR Amplifications and DNA Sequencing

PCR was performed according to the protocol of Expand High Fidelity PCR system (Hoffmann-La Roche). PCR products were cloned into pGEM-T Easy Vector (Promega) and transformed into XL-Blue–competent cells. Plasmids were purified with a Qiagen Spin Miniprep kit. DNA sequencing was performed in an ABI 3730 sequencer (Applied Biosciences) following the manufacturer's instructions. Primers used in this work are shown in Supplemental Table 9 online.

Sequence Analysis and Mapping of *TED* Insertion Sites

Sequences flanking *trTED* elements were isolated by iPCR and sequenced. In brief, genomic DNA was digested with *Bam*HI, *Eco*RI, *Hin*cII, *Hin*dIII, *Sac*I, or *Ssp*I and then ligated under dilute conditions to favor intramolecular ligation. PCR was performed as described above using appropriate *TED* primers. Unique PCR bands were directly sequenced without additional purification. Sequences flanking both ends were assembled into parental sequences by merging the identical 9-bp TSDs on either side. The assembled sequences were queried against the maize B73 RefGen_v2 (MGSC) database by BLASTN (Altschul et al., 1997) and manually annotated after downloading the BAC contig from the database and analyzing the coding capacity of sequences 10 kb upstream and downstream of the insertion by BLASTX.

TED-Like Transposon Annotation and Phylogenetic Analysis

The entire *TED* sequence was queried against the maize B73 RefGen_v2 (MGSC) database by BLASTN. Hits from the transposase coding region were chosen for further analysis. To define the TIRs of the putative transposons, flanking sequences 10 kb upstream and downstream of the matching region were retrieved from the B73 database and aligned against each other using NCBI-BLAST 2. *MULE* TIR sequences were identified from pairwise alignments and subsequently refined from the flanking TSDs. The newly identified *TED*-like elements were then subjected to the same sequence analyses as described above. The *TED* sequence was also queried against the *Sorghum* and *Brachypodium* databases at Phytozome (http://www.phytozome.net). Sequence features of *TED*-like elements were manually annotated to define TIRs, TSDs, and the coding capacity of the insertion sites as described above for maize. Transposases encoded by these elements were predicted with Fgenesh++ (http://linux1.softberry.com). The DDE domain was extracted from the predicted transposase by comparison with MURA and TEDA and used for phylogenetic analysis together with other reported DDE domain transposases (Yuan and Wessler, 2011). A phylogenetic tree was constructed using neighbor joining in MEGA version 5.05 (http://www.megasoftware.net/), with 1000 bootstrap replicates and the pairwise deletion option for handling gaps.

Accession Numbers

Sequence data from this article can be found in the GenBank/EMBL data libraries under the following accession numbers: *TED* sequence (GenBank KF287636), *bz-m175* allele (KF279654), *Bz* progenitor allele of *bz-m175* (KF279655), *Bz* High Loss allele (KF279653), and *Bz* High Knob allele (KF279652).

Supplemental Data

The following materials are available in the online version of this article.

Supplemental Figure 1. Positive Dosage Effect of the *bz-m175* Allele.

Supplemental Figure 2. *TED* Is a Low Copy Transposon in Maize and Its Grass Relatives.

Supplemental Figure 3. TED Dosage Effect.

Supplemental Figure 4. *trTED* Elements Maintain Their Transposase Activity.

Supplemental Figure 5. Sequence Features of *TED* Reinsertion Sites.

Supplemental Figure 6. Footprint Analysis of Somatic Excision Products from *bz-m175*.

Supplemental Figure 7. Detection of *TED* Somatic Reinsertions.

Supplemental Figure 8. Sequence Alignment of TIRs from *TED* at *bz-m175* and *TED*-Like Elements Isolated from *Zea nicaraguensis*.

Supplemental Figure 9. Duplicative Transposition of *TED* Elements.

Supplemental Figure 10. Sequence Analysis of Circular *TED* Elements.

Supplemental Figure 11. Phylogenetic Tree of *MULE* Transposases.

Supplemental Table 1. Segregation in Testcrosses of *Sh bz-m175*/*sh-bz-X3* Hemizygotes.

Supplemental Table 2. Germinal *TED* Transposition Sites Recovered via Inverse PCR Amplification.

Supplemental Table 3. Sequence Features of *dTED* and *fTED* Elements in bz-s Derivatives from *bz-m175*.

Supplemental Table 4. Somatic *TED* Reinsertion Sites Isolated by iPCR in Genomic DNA of Leaf Tissues.

Supplemental Table 5. *TED*-Related Elements Recovered via iPCR Amplification from Different Maize Lines and Teosinte.

Supplemental Table 6. Frequencies of *trTED* Duplications in Female Parent.

Supplemental Table 7. Sequence Features of *cTED* and *cdTED* Elements in *TED*-Active Lines.

Supplemental Table 8. *MULE*s Detected with a TEDA Query in Representative Plant Genomes.

Supplemental Table 9. Oligonucleotide Primers for PCR and iPCR Analysis.

ACKNOWLEDGMENTS

We thank Qinghua Wang, Limei He, and Jun Huang for comments on the article, Xiuzhi Liu and Xiaofang Xue for help in the greenhouse and laboratory, and Marc Probasco for plant care. This article is dedicated to Manford Goh, one of our enthusiastic undergraduate field helpers, who passed away suddenly this year. Funding for this project was provided by the National Science Foundation (DBI-0929350) and the Waksman Institute.

AUTHOR CONTRIBUTIONS

Y.L. and H.K.D. designed the work, analyzed the data, and wrote the article. Y.L. and L.H. performed the research.

Received July 23, 2013; revised August 19, 2013; accepted August 23, 2013; published September 13, 2013.

REFERENCES

Ågren, J.A., and Wright, S.I. (2011). Co-evolution between transposable elements and their hosts: A major factor in genome size evolution? Chromosome Res. **19:** 777–786.

Alleman, M., and Freeling, M. (1986). The *Mu* transposable elements of maize: Evidence for transposition and copy number regulation during development. Genetics **112:** 107–119.

Altschul, S.F., Madden, T.L., Schäffer, A.A., Zhang, J., Zhang, Z., Miller, W., and Lipman, D.J. (1997). Gapped BLAST and PSI-BLAST: A new generation of protein database search programs. Nucleic Acids Res. **25:** 3389–3402.

Benito, M.I., and Walbot, V. (1997). Characterization of the maize *Mutator* transposable element MURA transposase as a DNA-binding protein. Mol. Cell. Biol. **17:** 5165–5175.

Bennetzen, J.L. (1996). The *Mutator* transposable element system of maize. Curr. Top. Microbiol. Immunol. **204:** 195–229.

Britt, A.B., and Walbot, V. (1991). Germinal and somatic products of *Mu1* excision from the *Bronze-1* gene of *Zea mays*. Mol. Gen. Genet. **227:** 267–276.

Chalvet, F., Grimaldi, C., Kaper, F., Langin, T., and Daboussi, M.J. (2003). *Hop*, an active *Mutator*-like element in the genome of the fungus *Fusarium oxysporum*. Mol. Biol. Evol. **20:** 1362–1375.

Chomet, P., Lisch, D., Hardeman, K.J., Chandler, V.L., and Freeling, M. (1991). Identification of a regulatory transposon that controls the *Mutator* transposable element system in maize. Genetics **129:** 261–270.

Conrad, L.J., Bai, L., Ahern, K., Dusinberre, K., Kane, D.P., and Brutnell, T.P. (2007). State II *dissociation* element formation following *activator* excision in maize. Genetics **177:** 737–747.

Cowperthwaite, M., Park, W., Xu, Z., Yan, X., Maurais, S.C., and Dooner, H.K. (2002). Use of the transposon *Ac* as a gene-searching engine in the maize genome. Plant Cell **14:** 713–726.

Curcio, M.J., and Derbyshire, K.M. (2003). The outs and ins of transposition: From mu to kangaroo. Nat. Rev. Mol. Cell Biol. **4:** 865–877.

Daley, J.M., Palmbos, P.L., Wu, D., and Wilson, T.E. (2005). Nonhomologous end joining in yeast. Annu. Rev. Genet. **39:** 431–451.

Delseny, M., Han, B., and Hsing, Y.Ie. (2010). High throughput DNA sequencing: The new sequencing revolution. Plant Sci. **179:** 407–422.

Dennis, E.S., Finnegan, E.J., Taylor, B.H., Peterson, T.A., Walker, A.R., and Peacock, W.J. (1988). Maize transposable elements: Structure, function, and regulation. In Plant Transposable Elements, O.E. Nelson, ed (New York: Plenum Press), pp. 101–113.

Dietrich, C.R., Cui, F., Packila, M.L., Li, J., Ashlock, D.A., Nikolau, B.J., and Schnable, P.S. (2002). Maize *Mu* transposons are targeted to the 5′ untranslated region of the *gl8* gene and sequences flanking *Mu* target-site duplications exhibit nonrandom nucleotide composition throughout the genome. Genetics **160:** 697–716.

Dooner, H.K., and Belachew, A. (1989). Transposition pattern of the maize element *Ac* from the *bz-m2(Ac)* allele. Genetics **122:** 447–457.

Doseff, A., Martienssen, R., and Sundaresan, V. (1991). Somatic excision of the *Mu1* transposable element of maize. Nucleic Acids Res. **19:** 579–584.

Du, C., Fefelova, N., Caronna, J., He, L., and Dooner, H.K. (2009). The polychromatic *Helitron* landscape of the maize genome. Proc. Natl. Acad. Sci. USA **106:** 19916–19921.

Eggleston, W.B., Alleman, M., and Kermicle, J.L. (1995). Molecular organization and germinal instability of *R-stippled* maize. Genetics **141:** 347–360.

Eisen, J.A., Benito, M.I., and Walbot, V. (1994). Sequence similarity of putative transposases links the maize *Mutator* autonomous element and a group of bacterial insertion sequences. Nucleic Acids Res. **22:** 2634–2636.

Fedoroff, N.V. (2012). Presidential address. Transposable elements, epigenetics, and genome evolution. Science **338:** 758–767.

Fernandes, J., Dong, Q., Schneider, B., Morrow, D.J., Nan, G.L., Brendel, V., and Walbot, V. (2004). Genome-wide mutagenesis of *Zea mays* L. using *RescueMu* transposons. Genome Biol. **5:** R82.

Feschotte, C., and Pritham, E.J. (2007). DNA transposons and the evolution of eukaryotic genomes. Annu. Rev. Genet. **41:** 331–368.

Galli, M., Theriault, A., Liu, D., and Crawford, N.M. (2003). Expression of the Arabidopsis transposable element *Tag1* is targeted to developing gametophytes. Genetics **165:** 2093–2105.

Gao, D. (2012). Identification of an active *Mutator*-like element (*MULE*) in rice (*Oryza sativa*). Mol. Genet. Genomics **287:** 261–271.

González, L.G., and Deyholos, M.K. (2012). Identification, characterization and distribution of transposable elements in the flax (*Linum usitatissimum* L.) genome. BMC Genomics **13:** 644.

Gorbunova, V., and Levy, A.A. (1997). Circularized *Ac/Ds* transposons: Formation, structure and fate. Genetics **145:** 1161–1169.

Gorbunova, V., and Levy, A.A. (2000). Analysis of extrachromosomal *Ac/Ds* transposable elements. Genetics **155:** 349–359.

Hershberger, R.J., Benito, M.I., Hardeman, K.J., Warren, C., Chandler, V.L., and Walbot, V. (1995). Characterization of the major transcripts encoded by the regulatory *MuDR* transposable element of maize. Genetics **140:** 1087–1098.

Hershberger, R.J., Warren, C.A., and Walbot, V. (1991). *Mutator* activity in maize correlates with the presence and expression of the

Mu transposable element *Mu9*. Proc. Natl. Acad. Sci. USA **88:** 10198–10202.

Holligan, D., Zhang, X., Jiang, N., Pritham, E.J., and Wessler, S.R. (2006). The transposable element landscape of the model legume *Lotus japonicus*. Genetics **174:** 2215–2228.

Hsia, A.P., and Schnable, P.S. (1996). DNA sequence analyses support the role of interrupted gap repair in the origin of internal deletions of the maize transposon, *MuDR*. Genetics **142:** 603–618.

Hua-Van, A., and Capy, P. (2008). Analysis of the DDE motif in the *Mutator* superfamily. J. Mol. Evol. **67:** 670–681.

Huang, J.T., and Dooner, H.K. (2012). The spectrum and frequency of self-inflicted and host gene mutations produced by the transposon Ac in maize. Plant Cell **24:** 4149–4162.

Hudson, M.E., Lisch, D.R., and Quail, P.H. (2003). The *FHY3* and *FAR1* genes encode transposase-related proteins involved in regulation of gene expression by the phytochrome A-signaling pathway. Plant J. **34:** 453–471.

Hughes, J., and Hughes, M.A. (1994). Multiple secondary plant product UDP-glucose glucosyltransferase genes expressed in cassava (*Manihot esculenta* Crantz) cotyledons. DNA Seq. **5:** 41–49.

Iltis, H.H., and Benz, B.F. (2000). *Zea nicaraguensis* (Poaceae), a new teosinte from Pacific coast Nicaragua. Novon **10:** 382–390.

Jiang, N., Bao, Z., Zhang, X., Eddy, S.R., and Wessler, S.R. (2004). *Pack-MULE* transposable elements mediate gene evolution in plants. Nature **431:** 569–573.

Kidwell, M.G. (2002). Transposable elements and the evolution of genome size in eukaryotes. Genetica **115:** 49–63.

Kunze, R., and Weil, C.F. (2002). The *hAT* and CACTA superfamilies of plant transposons. In Mobile DNA II, N.L. Craig, R. Craigie, M. Gellert, and A.M. Lambowitz, eds (Washington, D.C.: ASM Press), pp. 565–610.

Li, Y., and Dooner, H.K. (2009). Excision of *Helitron* transposons in maize. Genetics **182:** 399–402.

Li, Y., and Dooner, H.K. (2012). *Helitron* proliferation and gene-fragment capture. In Plant Transposable Elements: Impact on Genome Structure and Function, M.A. Gransbastien and J.M. Casacuberta, eds (Berlin: Springer-Verlag), pp. 193–227.

Li, Y., Wang, Q., Segal, G., and Dooner, H.K. (2013). Gene tagging with engineered *Ds* elements in maize. In Methods in Molecular Biology: Plant Transposable Elements, T. Peterson, ed (New York: Springer Science+Business Media), pp. 83–99.

Lisch, D. (2002). *Mutator* transposons. Trends Plant Sci. **7:** 498–504.

Lisch, D., Chomet, P., and Freeling, M. (1995). Genetic characterization of the *Mutator* system in maize: Behavior and regulation of *Mu* transposons in a minimal line. Genetics **139:** 1777–1796.

Lisch, D., Girard, L., Donlin, M., and Freeling, M. (1999). Functional analysis of deletion derivatives of the maize transposon *MuDR* delineates roles for the MURA and MURB proteins. Genetics **151:** 331–341.

Lisch, D., and Jiang, N. (2009). *Mutator* and *MULE* transposons. In Handbook of Maize: Genetics and Genomics, J.L. Bennetzen and S. Hake, eds (New York: Springer), pp. 277–306.

May, B.P., Liu, H., Vollbrecht, E., Senior, L., Rabinowicz, P.D., Roh, D., Pan, X., Stein, L., Freeling, M., Alexander, D., and Martienssen, R. (2003). Maize-targeted mutagenesis: A knockout resource for maize. Proc. Natl. Acad. Sci. USA **100:** 11541–11546.

McCarty, D.R., Carson, C.B., Stinard, P.S., and Robertson, D.S. (1989). Molecular analysis of *viviparous-1*: An abscisic acid-insensitive mutant of maize. Plant Cell **1:** 523–532.

McCarty, D.R., et al. (2005). Steady-state transposon mutagenesis in inbred maize. Plant J. **44:** 52–61.

McVey, M., and Lee, S.E. (2008). MMEJ repair of double-strand breaks (director's cut): Deleted sequences and alternative endings. Trends Genet. **24:** 529–538.

Mottinger, J. (1973). Unstable mutants of *bronze* induced by premeiotic X-ray treatment in maize. Theor. Appl. Genet. **43:** 190–195.

Nassif, N., Penney, J., Pal, S., Engels, W.R., and Gloor, G.B. (1994). Efficient copying of nonhomologous sequences from ectopic sites via P-element-induced gap repair. Mol. Cell. Biol. **14:** 1613–1625.

Offen, W., Martinez-Fleites, C., Yang, M., Kiat-Lim, E., Davis, B.G., Tarling, C.A., Ford, C.M., Bowles, D.J., and Davies, G.J. (2006). Structure of a flavonoid glucosyltransferase reveals the basis for plant natural product modification. EMBO J. **25:** 1396–1405.

Qin, M.M., Robertson, D.S., and Ellingboe, A.H. (1991). Cloning of the *Mutator* transposable element *MuA2*, a putative regulator of somatic mutability of the *a1-Mum2* allele in maize. Genetics **129:** 845–854.

Radice, A.D., and Emmons, S.W. (1993). Extrachromosomal circular copies of the transposon *Tc1*. Nucleic Acids Res. **21:** 2663–2667.

Raizada, M.N., Nan, G.L., and Walbot, V. (2001). Somatic and germinal mobility of the *RescueMu* transposon in transgenic maize. Plant Cell **13:** 1587–1608.

Ralston, E.J., English, J., and Dooner, H.K. (1987). Stability of deletion, insertion and point mutations at the *bronze* locus in maize. Theor. Appl. Genet. **74:** 471–475.

Rhoades, M.M., and Dempsey, E. (1982). The induction of mutable systems in plants with the high-loss mechanism. Maize Genetics Coop. Newslet. **56:** 21–26.

Robertson, D.S. (1978). Characterization of a *Mutator* system in maize. Mutat. Res. **51:** 21–28.

Robertson, D.S. (1986). Genetic studies on the loss of *mu* mutator activity in maize. Genetics **113:** 765–773.

Robertson, D.S., and Stinard, P.S. (1989). Genetic analyses of putative two-element systems regulating somatic mutability in *Mutator*-induced aleurone mutants of maize. Dev. Genet. **10:** 482–506.

Roth, D.B., Porter, T.N., and Wilson, J.H. (1985). Mechanisms of nonhomologous recombination in mammalian cells. Mol. Cell. Biol. **5:** 2599–2607.

Rubin, E., and Levy, A.A. (1997). Abortive gap repair: Underlying mechanism for *Ds* element formation. Mol. Cell. Biol. **17:** 6294–6302.

Schnable, P.S., Peterson, P.A., and Saedler, H. (1989). The *bz-rcy* allele of the *Cy* transposable element system of *Zea mays* contains a *Mu*-like element insertion. Mol. Gen. Genet. **217:** 459–463.

Schnable, P.S., et al. (2009). The B73 maize genome: Complexity, diversity, and dynamics. Science **326:** 1112–1115.

Shepherd, N.S., Rhoades, M.M., and Dempsey, E. (1989). Genetic and molecular characterization of *a-mrh-Mrh*, a new mutable system of *Zea mays*. Dev. Genet. **10:** 507–519.

Singer, T., Yordan, C., and Martienssen, R.A. (2001). Robertson's *Mutator* transposons in *A. thaliana* are regulated by the chromatin-remodeling gene *Decrease in DNA Methylation* (*DDM1*). Genes Dev. **15:** 591–602.

Slotkin, R.K., Vaughn, M., Borges, F., Tanurdzić, M., Becker, J.D., Feijó, J.A., and Martienssen, R.A. (2009). Epigenetic reprogramming and small RNA silencing of transposable elements in pollen. Cell **136:** 461–472.

Sundaresan, V., and Freeling, M. (1987). An extrachromosomal form of the *Mu* transposons of maize. Proc. Natl. Acad. Sci. USA **84:** 4924–4928.

Swigonová, Z., Lai, J., Ma, J., Ramakrishna, W., Llaca, V., Bennetzen, J.L., and Messing, J. (2004). Close split of sorghum and maize genome progenitors. Genome Res. **14** (10A)**:** 1916–1923.

van Luenen, H.G., Colloms, S.D., and Plasterk, R.H. (1993). Mobilization of quiet, endogenous *Tc3* transposons of *Caenorhabditis elegans* by forced expression of *Tc3* transposase. EMBO J. **12:** 2513–2520.

Vitte, C., and Bennetzen, J.L. (2006). Analysis of retrotransposon structural diversity uncovers properties and propensities in angiosperm genome evolution. Proc. Natl. Acad. Sci. USA **103:** 17638–17643.

Vollbrecht, E., et al. (2010). Genome-wide distribution of transposed dissociation elements in maize. Plant Cell **22:** 1667–1685.

Walbot, V., and Rudenko, G.N. (2002). *MuDR*/*Mu* transposable elements of maize. In Mobile DNA II, N.L. Craig, R. Craigie, M. Gellert, and A.M. Lambowitz, eds (Washington, D.C.: ASM Press), pp. 533–564.

Wessler, S., Tarpley, A., Purugganan, M., Spell, M., and Okagaki, R. (1990). Filler DNA is associated with spontaneous deletions in maize. Proc. Natl. Acad. Sci. USA **87:** 8731–8735.

Wessler, S.R. (2006). Transposable elements and the evolution of eukaryotic genomes. Proc. Natl. Acad. Sci. USA **103:** 17600–17601.

Wicker, T., et al. (2007). A unified classification system for eukaryotic transposable elements. Nat. Rev. Genet. **8:** 973–982.

Williams, W.M., Satyanarayana, K.V., and Kermicle, J.L. (1984). *R-stippled* maize as a transposable element system. Genetics **107:** 477–488.

Xu, Z., Yan, X., Maurais, S., Fu, H., O'Brien, D.G., Mottinger, J., and Dooner, H.K. (2004). *Jittery*, a *Mutator* distant relative with a paradoxical mobile behavior: Excision without reinsertion. Plant Cell **16:** 1105–1114.

Yan, X., Martínez-Férez, I.M., Kavchok, S., and Dooner, H.K. (1999). Origination of *Ds* elements from *Ac* elements in maize: Evidence for rare repair synthesis at the site of *Ac* excision. Genetics **152:** 1733–1740.

Yuan, Y.W., and Wessler, S.R. (2011). The catalytic domain of all eukaryotic cut-and-paste transposase superfamilies. Proc. Natl. Acad. Sci. USA **108:** 7884–7889.